

On the Deformed Microstructure of Rolled Mg-2.9Y

S. A. Farzadfar¹, M. Sanjari¹, I.-H. Jung¹, E. Essadiqi² and S. Yue¹

¹McGill University, Department of Materials Engineering, Montreal, QC, Canada

²CANMET- Materials Technology Laboratory, Hamilton, ON, Canada

Keywords: Magnesium, Yttrium, Rolling, Texture

Abstract

The hot and cold rolled microstructures of a Mg-2.9Y alloy were examined by means of metallography, X-ray texture measurement and EBSD technique. It is found that Y in solid solution suppresses dynamic recrystallization even at 450 °C. After rolling, a heterogeneous microstructure containing twins and bands is obtained. The bands were found to originate from double and compression twins, and are locations of high-stored energy. The bulk texture of the rolled material consists of the typical basal component, and also a component from the ND towards the TD. The latter component results from the presence of parent grains with *c*-axis along the TD. The strain is accommodated in such parent grains by extension twinning and possibly prismatic slip.

Introduction

Available Mg sheets do not currently exhibit the room-temperature formability required in automotive applications. This is the main reason which retards the industrial application of this lightest structural material [1]. In rolled Mg alloy sheets, a strong basal texture develops, in which the basal planes are mainly distributed parallel to the RD-TD plane, where the RD and TD are rolling and transverse directions [2-4]. The basal texture develops mainly because of the dominant role played by basal slip and {10.2} extension twinning during deformation. These two mechanisms align the *c*-axis of grains with the direction of compressive strain, i.e., in rolled sheets, *c*-axes align with the ND (normal direction).

The presence of basal texture limits the room-temperature formability due to the restricted activities of <a> type slip systems under loading in the sheet normal and planar directions. Furthermore, the polarity of mechanical twinning in Mg results in the asymmetry of tension-compression strength in a textured material. It is therefore necessary to provide a way of weakening the texture in wrought Mg alloys.

It has recently been found that the addition of rare earth (RE) elements, such as Y, leads to significantly weaker textures [5-8]. One approach to study the effect of RE elements is by selecting binary Mg-RE alloys with the pure RE element in solid solution. Among the RE elements, Y is of particular interest due to its large solubility in Mg solid solution (2.2 wt% at 200 °C, and maximum solubility of 12 wt% at 567 °C) [9]. Very little data is available on the rolled microstructure of solid solution Mg-Y alloys [6, 10-12]. Some of these studies have been performed only on cold-rolled material that was pre-deformed by hot rolling [10, 12]. In other works [6, 11], the temperatures of pre/post-deformation annealing are dissimilar from that of deformation, which could result in precipitation (or dissolution of precipitates) and therefore variation in solute amount. A solid solution alloy, both before and

during deformation, is therefore required to investigate the effect of Y solute.

The objective of this study is to characterize the as-rolled microstructure of a solid solution Mg-Y alloy at room temperature, 350 °C and 450 °C. More emphasis will be put on the microstructure features after hot rolling.

Experimental Procedure

To avoid precipitation during hot rolling, a Mg-Y solid solution alloy with 2.9 wt% of Y was chosen. This composition was selected to ensure that solubility limit at the lowest hot rolling temperature (≈ 5.4 wt% at 350 °C) is not reached. The Mg-2.9Y alloy was prepared from high purity elements 99.9% Mg, 99.99% Zn, and 99.9% Y (all concentrations are given in wt%) by induction melting under SF₆ and CO₂ gas mixture. The molten alloys were cast into plates 100 mm in width and 6 mm in thickness in a steel mould pre-heated at 400 °C. Inductively coupled plasma atomic emission spectroscopy (ICP-AES) was used to determine the composition of the cast material, which was close to the nominal one (-0.12 wt% maximum difference). The major impurity levels were 0.03 wt% for Al and Fe, and 0.004 wt% for Si and Mn. To obtain solid solution alloys prior to rolling, the cast plates were heat treated at 430 °C for 24 h [13]. The average grain size in heat-treated cast material, measured by linear intercept method (ASTM standard E112), is 163(± 10) μm . Hot rolling at two temperatures, 350 °C and 450 °C, and cold rolling at room temperature were carried out in this work. The hot rolling was performed to 50% reduction in one pass to avoid inter-pass heating and possible meta-dynamic or static recrystallization. This is important since this study aims at clarifying the role of dynamic recrystallization on texture, and therefore any form other recrystallization types must be avoided. For rolling at room temperature, 30% reduction was successfully applied in 5 passes without major cracking. Minor edge cracking occurred at all rolling temperatures. Rolling was performed using laboratory rolling mills with a diameter of 150 mm and a rolling speed of 25 rpm. For hot rolling, the plates were pre-heated for 15 min prior to deformation, and quenched into room-temperature water within 1 s after rolling.

All microstructural and texture examinations were performed in the plane containing the RD and ND. The samples were ground down to 1200 grit SiC paper, and polished with 3 μm and 1 μm diamond suspension followed by 0.04 μm colloidal silica (Struers OP-S) polishing. In preparation for optical microscopy and electron back-scattered diffraction (EBSD), the polished samples were electropolished in 10% Nital solution at 20 V and temperatures ranging from -30 °C to -20 °C. For metallography, the samples were then etched with acetic picral (30 ml acetic acid, 15 ml H₂O, 6 g picric acid, 100 ml ethanol) for 3 to 5 s.

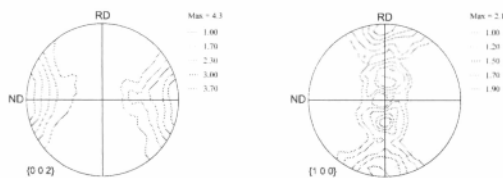
The macro-texture was evaluated by XRD technique using a Bruker D8 diffractometer with a Co K α source. The orientation distribution function (ODF) was constructed from the incomplete pole figures of {10.0}, {00.2}, and {10.1}. Recalculated pole figures were then derived from the ODFs. Micro-texture was studied via EBSD technique in a Hitachi S 3000 FE-SEM fitted with a TSL EBSD camera operating at 20 kV, 70° tilt angle and a step size of 0.3 μ m. The color format of EBSD maps is available on the CD version of the paper.

Results and Discussion

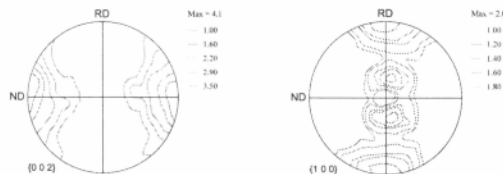
Macro-texture

The as-rolled macro-textures at different temperatures are shown in Figure 1 by (00.2) and (10.0) pole figures (PFs).

Room temperature



350 °C



450 °C

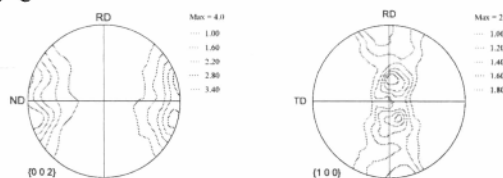


Figure 1. X-ray bulk texture after rolling at room temperature, 350 °C and 450 °C given by (00.2) and (10.0) PFs.

The as-rolled texture contains the typical strong basal component with the same value of maximum intensity in basal PFs at all temperatures. It should be mentioned that the average error in the maximum intensity of basal PFs is $\pm 12\%$.

Two off-basal texture components, visible in the basal PFs, are also present: (i) ND-RD component in which *c*-axes are rotated towards the RD, and (ii) ND-TD component in which *c*-axes are tilted towards the TD. The intensity of the latter component ranges from 1.6 to 1.8 MROD (multiples of a random orientation distribution). It is noteworthy to mention that despite lower reduction at room temperature, the general features of the texture as well as the maximum intensity of basal PFs is similar to those at 350 °C. At 450 °C, the basal PF exhibits a double-peak shape,

which could result from the possible activity of $\langle c + a \rangle$ slip system [2].

Microstructure

The as-rolled microstructure of the Mg-2.9Y alloy at 450 °C is shown in Figure 2.

The interesting feature of the microstructure is the absence of dynamic recrystallization (DRX) even at 450 °C. This was found after close examination of high-stored energy locations such as twins, twin intersections, and bands. The suppression of DRX in the presence of Y has recently been observed [8].

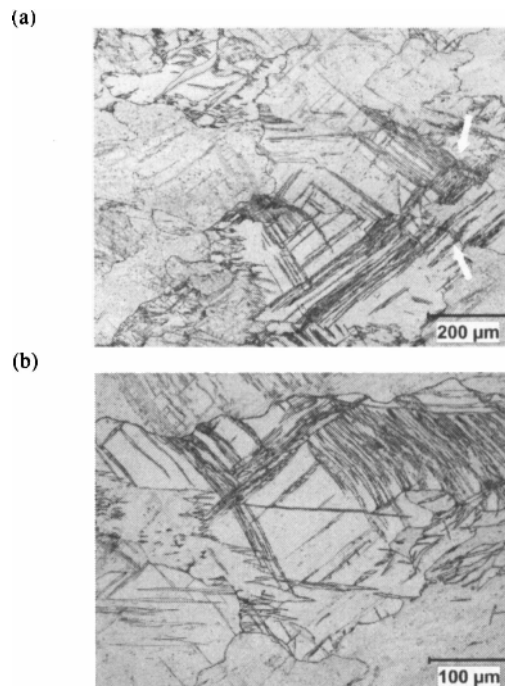


Figure 2. Optical micrographs of the as-rolled Mg-2.9Y alloy at 450 °C in RD-ND plane (RD is horizontal) from the center of sheets.

The role of Y in DRX suppression is not yet known, but is believed to be related to a change in the atomic potential. This change could possibly alter the lattice friction and consequently the critical resolved shear stress (CRSS) of slip systems. Another possibility is the pinning effect of Y on boundaries (low angle and high angle), which prevents recrystallization.

Twins with both thin and thick morphologies have evolved during deformation (Figure 2(b)). The thin twins, which are most probably contraction and/or double twins [14], pass sometimes through several grains, as is highlighted by arrows in Figure 2(a). The microstructure features at 350 °C and room temperature are similar to those at 450 °C.

Micro-texture

To enhance the EBSD indexing, the as-rolled material was annealed for 3 min at 400 °C, and the obtained microstructures are depicted in Figure 3. High-angle boundaries (HABs with $\theta > 15^\circ$) are shown by black lines.

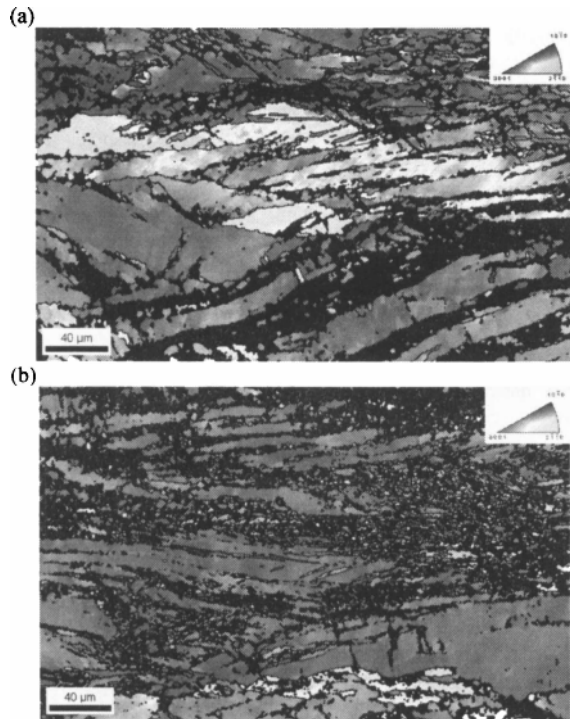


Figure 3. EBSD map (referring to the ND) after rolling at 350 °C (a) and 450 °C (b) followed by annealing at 400 °C for 3 min, showing band-like structures. The maps show the RD-ND plane with the RD being horizontal.

Un-indexed regions appearing in band-like structure are observable, which are most probably zones of deformation localization. Note that the short annealing treatment initiated formation of new grains at the bands. The bands, observed at all rolling temperatures, appear either at 30-40° from the RD or horizontally along the RD. The microstructure examination revealed that the horizontal bands are majorly limited to one basal parent grain, and do not pass through several grains. An example of horizontal bands is shown in Figure 4.



Figure 4. EBSD map (referring to the ND) after rolling at 450 °C (followed by annealing at 400 °C for 3 min) showing horizontal bands in basal parent grains. The maps show the RD-ND plane with the RD being horizontal.

The bands contain mainly compression and double twins as is evidenced by different types of twin boundary shown in Figure 5. The image quality (IQ) map of the microstructure region shown in Figure 3(a) is given in Figure 5 along with the length fraction of each twin boundary.

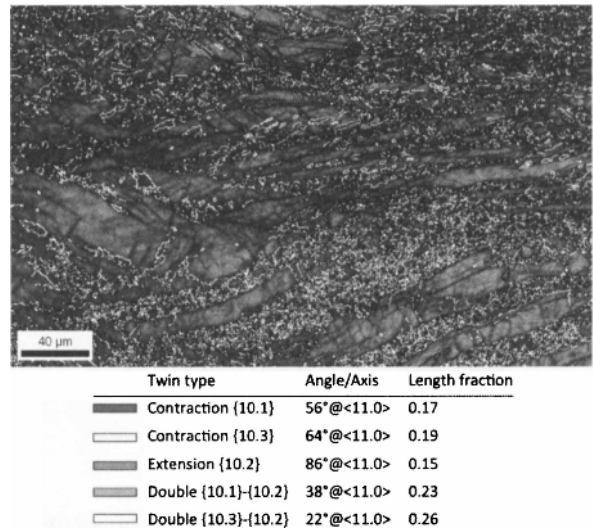


Figure 5. IQ map of the microstructure region illustrated in Figure 3(a). The boundaries corresponding to different twin types are also shown.

As can be seen in Fig. 5, two types of contraction twinning, {10.1} and {10.3}, extension twinning {10.2}, and two types of double twinning, {10.1}-{10.2} and {10.3}-{10.2}, are present. The bands, and noticeably the large one at the bottom of the map, contain mainly boundaries corresponding to double twinning. This is evidenced by their larger fraction compared to that of contraction and extension twins, i.e. 0.23 in the case of {10.1}-{10.2} twinning and 0.26 in the case of {10.3}-{10.2} twinning. The contraction (red and yellow boundaries) and extension (orange boundaries) twins, detected on the IQ map, are parts of the above-mentioned double twins. This is illustrated in Figure 6 by a detailed description of different twin boundaries for the rolled material at 450 °C.

A white arrow on Figure 6(b) highlights a white boundary pertaining to a {10.3}-{10.2} double twin. The upper boundary of this twin has formed by {10.3} contraction twinning (yellow boundary) and {10.2} extension twinning (orange boundary). This example illustrates the connection between double twinning and the constituent contraction and extension twinning. In other words, double twinning occurs when the matrix twins along either {10.1} or {10.3} plane, and then the twinned region twins along {10.2} plane. Therefore, when double twins are detected, the constituent primary twins are also present in the microstructure. As can be seen in Figure 6(a), un-indexed parts exist inside the twins near the white arrow, which are indicative of deformation localization at these twins, and most probably the mechanism by which the bands form with straining. As a result of double twinning, unfavorably oriented basal planes reorient to a more favorable orientation (38° and 22° reorientation after {10.1}-{10.2} and {10.3}-{10.2} double twinning, respectively), which could accommodate further strain.

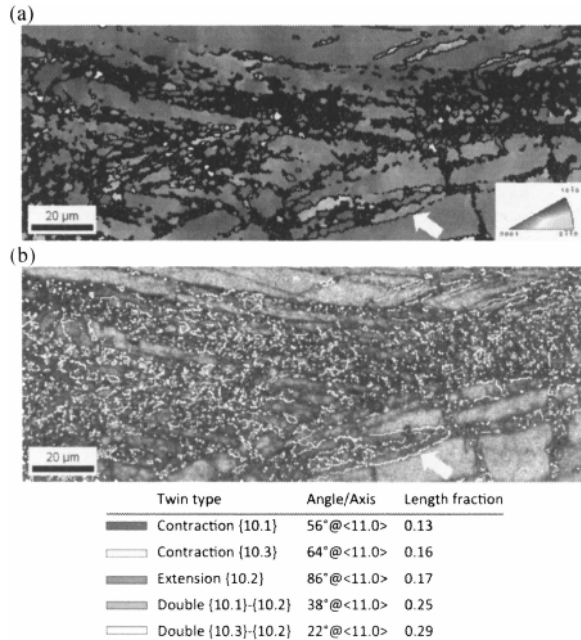


Figure 6. EBSD map (referring to the ND) of the rolled material at 450 °C, and the corresponding IQ map with different twin boundaries, showing the presence of contraction and double twins.

At all rolling temperatures, the parent grains were found to possess two different orientations: (i) the typical basal orientation (colored in red in Figure 7), or (ii) an orientation with *c*-axis along the TD (colored in green in Figure 7). The latter orientation pertains to the ND-TD component of the bulk texture displayed in Figure 1, and the parent grains possessing such orientation are hereafter termed ND-TD (parent) grains.

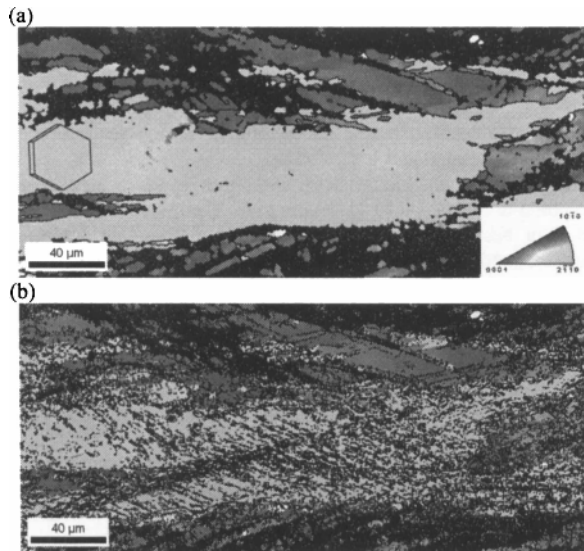


Figure 7. EBSD map of the as-rolled microstructure at 350 °C in RD-ND plane (RD is horizontal), HABS (a) and LABs (b) are shown separately on the EBSD map for clarity.

The LABs within ND-TD parent grains (Figure 7(b)) are essentially straight lines that intersect at an angle of approximately 120°, and coincide with the trace of prismatic planes as is illustrated by the hexagonal unit cell in Figure 7(a). These observations indicate the possible activity of prismatic slip. The orientation of ND-TD grains is also favorable for extension twinning. The upper area of the ND-TD grain in Figure 7(a) seems to be twinned parts because of both (near-)basal orientation and morphology of these regions. It is therefore believed that extension twinning is another mode of deformation accommodation in ND-TD parent grains. All the above-mentioned findings suggest that ND-TD grains are in fact the initial parent grains, which formed during casting, and that their orientation is preserved by the activation of prismatic slip. Work is ongoing to identify the origin and type of slip system activated in ND-TD grains.

Summary

The as-rolled microstructure of a solid solution Mg-2.9Y alloy was characterized. It was found that Y in solid solution suppresses dynamic recrystallization even at 450 °C. The unrecrystallized microstructure consists of twins and bands. The bands were found to originate from double and compression twins, and are locations of high-stored energy. The bulk texture of the rolled material exhibits the typical basal component, and an ND-TD component. The latter results from the presence of parent grains with *c*-axis along the TD. The strain is accommodated in such parent grains by extension twinning and possibly prismatic slip.

References

- [1] K.U. Kainer, *Magnesium Alloys and Technologies* (Weinheim: Wiley-VCH, 2003).
- [2] S.R. Agnew, M.H. Yoo, C.N. Tomé, "Application of Texture Simulation to Understanding Mechanical Behavior of Mg and Solid Solution Alloys Containing Li or Y," *Acta Mater.*, 49 (2001) 4277-4289.
- [3] M.R. Barnett, M.D. Nave, C.J. Bettles, "Deformation Microstructures and Textures of Some Cold Rolled Mg Alloys," *Mater. Sci. Eng. A*, 386 (2004) 205-211.
- [4] A. Jager, P. Lukac, V. Gartnerova, J. Haloda, M. Dopita, "Influence of Annealing on the Microstructure of Commercial Mg Alloy AZ31 after Mechanical Forming," *Mater. Sci. Eng. A*, 432 (2006) 20-25.
- [5] J. Bohlen, M.R. Nürnberg, J.W. Senn, D. Letzig, S.R. Agnew, "The Texture and Anisotropy of Magnesium-Zinc-Rare Earth Alloy Sheets," *Acta Mater.*, 55 (2007) 2101-2112.
- [6] K. Hantzsche, J. Bohlen, J. Wendt, K.U. Kainer, S.B. Yi, D. Letzig, "Effect of Rare Earth Additions on Microstructure and Texture Development of Magnesium Alloy Sheets," *Scripta Mater.*, 63 (2010) 725-730.
- [7] N. Stanford, "Micro-alloying Mg with Y, Ce, Gd and La for Texture Modification—A Comparative Study," *Mater. Sci. Eng. A*, 527 (2010) 2669-2677.
- [8] S. Yi, D. Letzig, K. Hantzsche, R.G. Martinez, J. Bohlen, I. Schestakow, S. Zaeferrer, "Improvement of magnesium sheet formability by alloying addition of rare earth elements," *Mater. Sci. Forum*, 638-642 (2010) 1506-1511.
- [9] L.L. Rokhlin, *Magnesium Alloys Containing Rare Earth Metals* (London: Taylor & Francis, 2003).

- [10] R. Cottam, J. Robson, G. Lorimer, B. Davis, "Texture Evolution During the Static Recrystallization of Three Binary Mg-Y Alloys," *Ceram. Trans.*, 200 (2008) 501-508.
- [11] R. Cottam, J. Robson, G. Lorimer, B. Davis, "Dynamic Recrystallization of Mg and Mg-Y Alloys: Crystallographic Texture Development," *Mater. Sci. Eng. A*, 485 (2008) 375-382.
- [12] S. Sandlöbes, S. Zaeferrer, I. Schestakow, S. Yi, R. Gonzalez-Martinez, "On the Role of Non-basal Deformation Mechanisms for the Ductility of Mg and Mg-Y Alloys," *Acta Mater.*, 59 (2011) 429-439.
- [13] S.A. Farzadfar, M. Sanjari, I.-H. Jung, E. Essadiqi, S. Yue, "Role of Yttrium in the Microstructure and Texture Evolution of Mg," *Mater. Sci. Eng. A*, 528 (2011) 6742-6753.
- [14] S.E. Ion, F.J. Humphreys, S.H. White, "Dynamic Recrystallisation and the Development of Microstructure During the High Temperature Deformation of Magnesium," *Acta Metall.*, 30 (1982) 1909-1919.